Electron-impact excitation at small scattering angles: The Lassettre limit and attendant normalization of measured relative differential cross sections

Z. Felfli, N. Embaye, P. Ozimba, and A. Z. Msezane
Department of Physics and Center for Theoretical Studies of Physical Systems, Clark Atlanta University, Atlanta, Georgia 30314
(Received 4 February 2000; published 12 December 2000)

The recent generalized Lassettre expansion (GLE) [Phys. Rev. Lett. **81**, 961 (1998)] employing only a single Regge pole is used to demonstrate the applicability of the Lassettre limit theorem over the entire electron impact energy without the involvement of the nonphysical region of the apparent generalized oscillator strength (AGOS). At forward scattering the GLE yields the unique long-sought-after normalization curve to the optical oscillator strength of the measured relative electron differential cross sections (DCS's) through the AGOS. Optically allowed transitions in H, He, Xe, and N_2O are used to illustrate the normalization procedure. We conclude that the GLE together with the momentum dispersion method of Haffad *et al.* [Phys. Rev. Lett 76, 2456 (1996)] now constitute a set of invaluable methods for use in guiding electron DCS measurements, including the identification of incorrectly normalized and/or spuriously behaved data in the difficult to measure small angular regime. It is hoped that this paper will inspire more measurements of DCS's at zero-angle scattering, since currently very few such measurements are available.

DOI: 10.1103/PhysRevA.63.012709 PACS number(s): 34.80.Dp, 31.50.Df, 32.70.Cs, 34.10.+x

I. INTRODUCTION

The niceties associated with the resolution of the long-standing problem of reaching the optical oscillator strength (OOS) limit, commonly known as the ''Lassettre limit theorem,'' when starting from any electron impact energy E, and the problem we have encountered with many reviewers, suggest that we first place the problem in perspective. Bethe [1] introduced the concept of the generalized oscillator strength (GOS) which directly manifests the atomic wave functions and the dynamics of atomic electrons. Miller and Platzman [2] recommended that important information can be obtained about both the electron differential cross sections (DCS's) and integral cross sections (ICS's) by examining the GOS as the momentum transfer squared, $K^2 \rightarrow 0$, and concluded that for $K^2 \ll 1$, the GOS converges to the OOS. The authors of Ref. [3] established that this must be valid regardless of E, viz. the applicability of the first Born approximation (FBA). Earlier, Bonham [4] predicted the existence of minima in the GOS function. The limiting behavior of the GOS as $K^2 \rightarrow 0$ was examined [5–7] with no clear departure from the limit theorem. One of the major theoretical difficulties limiting developments is that the value $K^2 = 0$ is nonphysical for finite E and, therefore, experimentally inaccessible. Consequently, an interpolation-extrapolation algorithm on the experimental data through the nonphysical region is necessary.

The limiting behavior of the GOS as $K^2 \rightarrow 0$ is important *inter alia* in normalizing the measured relative electron DCS's [8–11], the determination of OOS's from absolute DCS's [5,12–14], the calculation of cross sections for energy transfer in molecules [15], and the evaluation of the singlet-triplet energy differences [16,17] as well as ICS's [18]. One of the major problems encountered in extrapolating the measured GOS to the OOS, employing the standard Lassettre series [19], apart from the problem of convergence, has been that the nonphysical region of the GOS becomes extensive as E decreases toward threshold, thereby making the extrapolation difficult and unreliable [12]. Added to this, is that measurements tend to be riddled with errors at and near $\theta = 0°$. To remedy some of the problems, the Regge pole representation of the electron DCS was introduced [20]. The approach analytically continues the measured data from the larger angular region, where they are generally more reliably measured, through to zero scattering angle, where measurements are difficult to obtain.

The difficulties of measuring reliably the electron DCS's for atomic, ionic, and molecular transitions at small scattering angles including zero, well documented in the literature [12,21,22] are still clearly manifest even in the most recent measurements for H [23] and Li [24]. For the former, measurements were obtained down to only 7° at all the impact energies considered, while for the latter, data were obtained down to 6° at 21.8 eV. The same problem is exemplified for molecular transitions by the vibronic excitation bands ($\nu = 1-4$) of the $b\,^1\pi^u$ electronic state of N_2 [25], where data were obtained down to only 2.75° at 300 eV. Similarly, for the electron-impact excitation of the optically allowed transitions in Mg II, Zn II, and Cd II, the unmeasured angular regimes at 50 eV [21] are $0° \leqslant \theta < 4°$, $0° \leqslant \theta < 6°$, and $0° \leqslant \theta < 4°$, respectively.

Problems of determining absolute values of the measured electron DCS's using a GOS technique and contributions to the ICS's from the small angular regime were discussed by Ismail and Teubner [11], who measured the DCS's for excitation of the resonance transition in Cu down to $\theta = 2°$ at all their impact energies. They also demonstrated that at 20 and 100 eV 84% and 99%, respectively of the contributions to the ICS's come from the approximate angular range $0 \leqslant \theta < 15°$. This conclusion is consistent with the results found by Chen and Msezane [26] for optically allowed transitions in Xe and Na. Also, the contribution from the angular regime not covered by the measurement ($0 \leqslant \theta < 6°$) to the ICS's in the electron excitation of the states $6s[\frac{3}{2}]_{1,2}$ of Xe was found [12] to be between 1% and 70% for E values between 15 and 100 eV, respectively.

Above we have demonstrated sufficiently that many measurements of the electron DCS's for optically allowed transitions in atoms obtain data only down to some small angle θ_s near $\theta=0°$, and almost never at $\theta=0°$. (We note that the same applies to molecular transitions. The case of ionic transitions is even worse; there are very few measurements of DCS's for them because of severe technical difficulties). However, these transitions receive the major contribution to the ICS's mainly from the small angular range, particularly at high impact energies. Consequently, there is a great need to investigate the angular regime near and at $\theta=0°$, as well as the applicability of the Lassettre limit theorem for the normalization of the measured relative electron DCS's regardless of the electron-impact energy, the subject of this paper, to guide measurements. Several years ago the Atomic Theory Group at Clark Atlanta University, together with collaborators, embarked upon the development of innovative theoretical approaches for application to small-angle electron scattering. Here we will employ some of the methodologies to resolve the problem of reaching the Lassettre limit regardless of the electron impact energy and without traversing the nonphysical region of the GOS. Normalization curves will be extracted from the generalized Lassettre exposition (GLE), and illustrated using optically allowed transitions in H, He, Xe, and N_2O.

II. THEORY

A. Overview

Optically allowed transitions have long-range interaction potentials. Therefore, in calculating cross sections, many angular-momentum states must be considered. However, no physical understanding of the angular distribution is achieved through summing a partial wave series whose terms and number are significant [27]. The Regge pole representation of scattering problems embodies deep physical insights; it leads to a new physical interpretation of diffraction scattering [28]. The Regge pole representation of the electron DCS's makes use of a dynamical angular-momentum expansion in which the angular momenta are no longer integers, but their values depend drastically on the dynamics of the problem under investigation [29]. Such a representation results in an enormous gain because, while the ordinary kinematic angular momentum requires a significant number of partial waves when the energy increases from threshold, the dynamical Regge series requires less and less contributing terms. It is, therefore, the appropriate methodology for analyzing the medium to high electron scattering.

Recently, nonanalytic terms have been identified in the apparent generalized oscillator strength (AGOS) function near zero momentum transfer squared, coming from second-order long-range interaction potentials [30]. This result, combined with a single Regge pole [20], was used to obtain the generalized Lassettre expansion [30]. Used with the accurate electron DCS's of Ref. [31], the GLE yields outstanding OOS results for the H $1s$-$2p$ transition, down to electron-impact energy E near threshold. Consequently, embedded in the GLE is the long-sought-after normalization curve for the measured relative electron DCS's for optically allowed transitions. This curve, to be extracted and presented below, is compatible with the Lassettre limit theorem throughout the electron impact energy. This theorem has never been verified for non-Born transitions, although experimenters have long been attracted to utilizing it for normalizing the measured relative electron DCS's to the OOS's [8].

Since the main thrust of this paper is reaching the Lassettre limit of the GOS as $K^2\rightarrow 0$, the OOS, when starting from any electron-impact energy, and the extraction of the attendant normalization curve for the measured relative DCS's, we will need the three recent theoretical approaches: the momentum dispersion method (MDM) of Haffad *et al.* [20], the forward scattering function (FSF) of Ref. [32], and the GLE [30]. The utility of the MDM is in the determination of small-angle data where experiments experience difficulties measuring reliably through analytical continuation of the larger angular data which are generally measured more accurately by comparison, as well as the identification of spuriously behaved data at and near $\theta=0°$. The FSF is used to assess improper normalization of the measured relative electron DCS's through the GOS's. The presence of nonanalytic terms of the form $\sqrt{K^2}$ near $K^2=0$, coming from second-order long-range interaction, has led to the GLE. The GLE is useful for obtaining OOS's from absolute DCS's, and normalizing measured relative DCS's to the OOS. The three theoretical approaches are briefly described below.

B. Momentum dispersion method (MDM)

The DCS and GOS for atomic or molecular excitation by a fast electron are related through (atomic units are used throughout) [1,33]

$$f(E,K^2)=\frac{\omega}{2}\frac{k_i}{k_f}K^2\left(\frac{d\sigma}{d\Omega}\right), \tag{1}$$

where

$$K^2=2E\left[2-\frac{\omega}{E}-2\left(1-\frac{\omega}{E}\right)^{1/2}\cos\theta\right]; \tag{2}$$

ω, k_i, and k_f are, respectively, the excitation energy, the electron momenta before and after collision, K and θ are the momentum transfer and scattering angle, and E is the impact energy. We note that although Eq. (1) is obtained within the applicability of the FBA, an AGOS can be defined so that the energy-dependent equation (1) is also applicable when measured or calculated DCS's are used [33]. The limit of the AGOS as $K^2\rightarrow 0$ is

$$f^0=\lim_{K^2\rightarrow 0} f(E,K^2). \tag{3}$$

Ester and Kessler [12] found that for $E\leqslant 40$ eV their measured absolute data for the electron excitation of Xe to the states $6s[\frac{3}{2}]_{1,2}$ could not be extrapolated to the Lassettre limit, viz. the OOS, using the Lassettre formula [3,19]. Also, the problem associated with the normalization of the measured relative electron DCS's through the standard Lassettre expansion, particularly when using relatively small impact

energies, was discussed. Haffad *et al.* [20] discovered that the expansion coefficients in the Lassettre expansion increased dramatically with each new term, thereby limiting the utility of the expansion to only the generally more inaccurately measured small angular data. To circumvent this problem Haffad *et al.* used a dispersion relation representation of the DCS's for dipole allowed transitions at small-K^2 values. The Regge pole representation of the electron DCS's transforms Eq. (1) to [20]

$$F(x^2)=\frac{1}{(1+x^2)^6}[R+2r\cos(\varepsilon\log(1+x^2)-\phi)], \quad (4)$$

where $x=K/Y$, with $Y=\sqrt{2I}+\sqrt{2(I-\omega)}$, I and ω being the ionization and excitation energies, respectively. The quantities R, r, ε, and ϕ are yet to be determined. Equation (4) is mapped through

$$z=\log(1+x^2) \quad \text{and} \quad F^m(z)=(1+x^2)^6F(x^2), \quad (5)$$

which reduce it to

$$F^m(z)=a_0+a_1\cos\varepsilon z+b_1\sin\varepsilon z, \quad (6)$$

where $a_0=R$, $a_1=2r\cos\phi$ and $b_1=2r\sin\phi$. In the new system of variables the AGOS is expanded in a Fourier series, of which we have retained only the first terms determined from Eq. (6), and $\log(1+x^2)$ is a natural variable. The OOS is then

$$f^0=a_0+a_1. \quad (7)$$

The parameters a_0, a_1, b_1, and ε are determined by minimizing $F^m(z)$ through the functional

$$\mathcal{F}=\sum_{i=1}^{N}\left[\frac{F_i^{\text{exp}}-F^m(z_i)}{\Delta F_i^{\text{expt}}}\right]^2, \quad (8)$$

where N is the number of experimental data points, z_i, F_i^{exp}, and ΔF_i^{expt} are the mapped experimental values through the mapping [Eq. (5)] of the Nth point position, the AGOS value, and an error in the AGOS, respectively. The dependence of F^m on z is irrelevant to the outcome of the parameters. This is a very fine and desirable feature of the method because the investigations of F^m as a function of a new variable will not result in a new derivation, but only in a modification in the definition of both F^m and z. We stress that the OOS's are automatically extracted with the constants, a_0, a_1, b_1, and ϵ in the method. The correct OOS's therefore provide self-consistency checks of the measurements [34].

Equation (6) represents the expression for the MDM. In an appropriate representation the AGOS varies linearly with K^2, so that the difficult to measure smaller angular data can be obtained readily through analytical continuation. The MDM was used extensively to obtain smaller angular data from larger angular measurements and to calculate ICS's for transitions in Xe and N_2 [35].

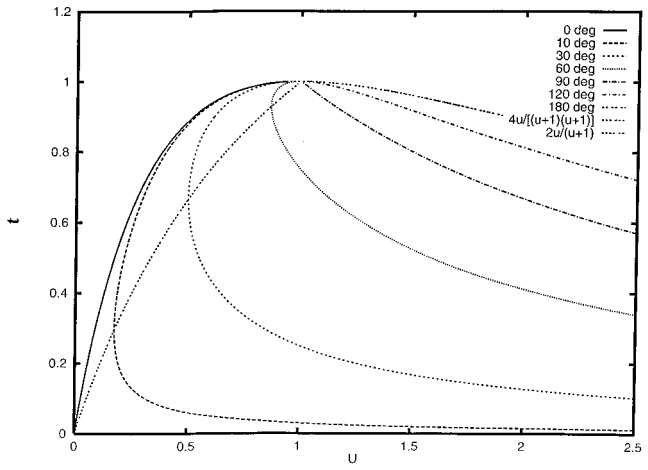

FIG. 1. Kinematics of the electron excitation process using dimensionless variables t and u. The curves, starting from the left, represent $\theta=0°$, 10°, 30°, 60°, 90°, 120°, and 180°, respectively. Note that the curve connecting the maxima is the envelope curve [32], and the $\theta=0°$ curve, the only fixed angle curve, continuously connects thresholds, $t=1$ and $t=0$ and has its maximum at $t=0$. All other curves for which $\theta\neq 0°$ avoid the limit point $t=0$ and $u=0$, corresponding to the optical oscillator strength.

C. Forward scattering function (FSF)

When the dimensionless variables

$$y=\cos\theta, \quad u=\frac{K^2}{2\omega} \quad \text{and} \quad t=\frac{\omega}{E} \quad (9)$$

are used, the expression for K^2 is transformed to

$$ut=2-t-2\sqrt{(1-t)}y, \quad (10)$$

where $0\leqslant t\leqslant 1$, $u\geqslant 0$, and y is without restriction. The physical region corresponds to $|y|\leqslant 1$, while $|y|>1$ defines the nonphysical region. At fixed y the energy parameter t has two values. When $u\sim 1$, they are

$$t_1=4u/(1+u)^2 \quad \text{and} \quad t_2=4\sin^2\theta/(1+u)^2. \quad (11)$$

Notably, t_1 is independent of θ, and corresponds to the forward scattering ($\theta=0°$) of the AGOS [32]; see Fig. 1. The dependence of t_2 on θ is weak at $\theta\sim 90°$. On the envelope curve [32] $t=2u/(1+u)$, i.e., $K^2=2\omega\sin\theta(u=\sin\theta)$, we have $t_1=t_2$. Figure 1 shows the variation of t with u for values of $\theta=0-180°$. Also plotted is the envelope curve; it joins the maxima of the curves. Interestingly, the maximum of the $\theta=0°$ curve is at $u=0$. Clearly, the only curves that continuously connect $E=\omega$ and $E=\infty$ (the OOS limit) are the forward-scattering and envelope curves. However, the forward-scattering curve is the only fixed angle curve that connects continuously the two energy limits. We note that $u\leqslant 0.5$ for values of t up to about 0.9, implying that u is a natural expansion variable even at fairly low electron-impact energies. This explains why sometimes first Born approximation is applicable even when E appears to be fairly low.

Thus, if the AGOS's are continuous functions of K^2 and E, they start to merge with the forward-scattering curve at

the energies corresponding to the envelope curve, i.e., $E < \omega(1+\sin\theta)/(2\sin\theta)$ for $\theta < 90°$. All other curves corresponding to $\theta > 90°$ merge with the forward-scattering curve at $E=\omega$. The closer θ is to 90°, the less the curves depend on the scattering angles. The point $u=K^2/2\omega$, $E=\omega$, and $\theta=90°$ is a point of concentration of the AGOS as a function of E or K^2. The point $u=0(K^2=0)$, $E=\infty$ admits only the angle $\theta=0°$, corresponding to the OOS; all other angles are excluded. The interest here is in the small-angle scattering, roughly $\theta \leqslant 15°$.

Equations (9) and (10) have been used to obtain the FSF [32],

$$\Phi(u) = f^0\left[1 - \frac{u}{u_{\max}}\right]\exp -(u/u_{\max})^2, \tag{12}$$

where $u_{\max}=0.25$, and f^0 is the OOS. Equation (12) describes the locus of the $\theta=0°$ AGOS points at various E values, with $E_{\min} \cong 2.5\omega$, such that $t=4u/(1+u)^2$. For any optically allowed transition, $\Phi(u)$ can be obtained from that of the H $1s$-$2p$ transition (or any other accurately known transition) and the corresponding OOS's [32]. The FSF and MDM have been used together to normalize measured relative electron DCS's [36–39], and to identify spurious behavior in both measured and calculated DCS's at and near $\theta=0$ [40,41]. Recently, the FSF was generalized [42] for use in the normalization of the relative experimental excitation or ionization DCS's or DDCS's. The new normalization [42] is effected beyond the FBA, and without extrapolation through the nonphysical region.

D. Generalized Lassettre expansion (GLE)

At low electron-impact energy, only a few partial waves are necessary to represent a scattering process correctly. When increasing the energy, more and more waves contribute to the general process, and the partial-wave expansion converges slower and slower. In particular, the presence of a square-root singularity at $K^2=0$, prevents the partial wave expansion from converging there. Regge [29] proposed using *complex angular momenta* to produce a representation that converges for *nonphysical* transfer momenta. In this representation the amplitude is expanded into *generalized* partial waves:

$$g(E,\cos\theta) = \sum_{\nu} (2\nu+1) f_\nu(E) P_\nu(\cos\theta). \tag{13}$$

The angular momenta $\nu(E)$ are no longer the universal *kinematical* integer angular momenta, but complex numbers that are *energy dependent* and are called Regge poles. $P_\nu(\cos\theta)$ are the Legendre functions of the first kind that reduce to the ordinary Legendre polynomials when $\nu(E)$ becomes an integer. $\nu(E)$ depends explicitly on the precise dynamics of the system under investigation, and can be computed from first principles using the Schrödinger equation. Recently, a general method of calculating Regge poles for both singular and regular potentials was developed and illustrated [43,44].

The transcendental functions $P_\nu(\cos\theta)$ are not of immediate use, and Eq. (13) can be replaced by a similar one without loss of generality [20],

$$g(E,\cos\theta) = \sum_{\nu} \frac{\rho_\nu(E)}{(1+x^2)^{-\nu}}, \tag{14}$$

where $x^2=K^2/Y^2$ is a linear function of $\cos\theta$ at *fixed energy*. The set $\nu(E)$ is the same in both Eqs. (13) and (14). What are the advantages of the formula represented by Eq. (13) or Eq. (14) over the traditional angular momenta expansion? We list the main ones.

(1) The Regge expansion will converge outside the physical region, and, in particular, for nonphysical scattering angles as in the case where one has to extrapolate the AGOS to obtain the OOS corresponding to a nonphysical value (purely imaginary) of the scattering angle.

(2) One of the most remarkable general property of the Regge poles $\nu(E)$ is that when $E \to +\infty$, they tend toward negative integers. For the $s \to p$ dipole-allowed transition, the value is -3, corresponding to the *leading* Regge pole (the one with the largest real part; we call this the Lassettre pole).

(3) For large physical energy, the real part of $\nu(E)$ behaves like

$$\mathrm{Re}(\nu(E)) \sim -3 + \frac{C}{E\ln E}. \tag{15}$$

This real part controls the fast decrease of the cross section with increasing momentum transfer.

(4) For large physical energy, the imaginary part of $\nu(E)$ behaves like

$$\mathrm{Im}(\nu(E)) \sim \frac{C'}{\sqrt{E}}. \tag{16}$$

This imaginary part controls the oscillations of the cross section at large momentum transfer.

In the present case, where we analyze a K^2 region *before the first minimum*, we can neglect the imaginary part of the leading Regge pole (that controls the oscillations in the DCS and write the GLE with only one Regge pole) [30]

$$f(E,K^2) = \frac{f^0}{(1+x)^6} + A\frac{\omega}{E}\frac{\sqrt{x}}{(1+x)^{\nu(E)}}, \tag{17}$$

where the OOS and A do not depend on energy, and where

$$\nu(E) = 6 + \frac{C}{(E/\omega)\ln(E/\omega)}. \tag{18}$$

Equation (15) can be derived by computing the next order term in expansion (8-4) in Ref. [29]. The constant C could be computed knowing the behavior at small distances of the corresponding effective potential, and C' is simply related to C. Alternatively, the constant C can be computed directly from the Schrödinger equation through the general expressions given in Refs. [43, 44] with the appropriate potentials used. Equations (17) and (18) give a *global analysis* of the

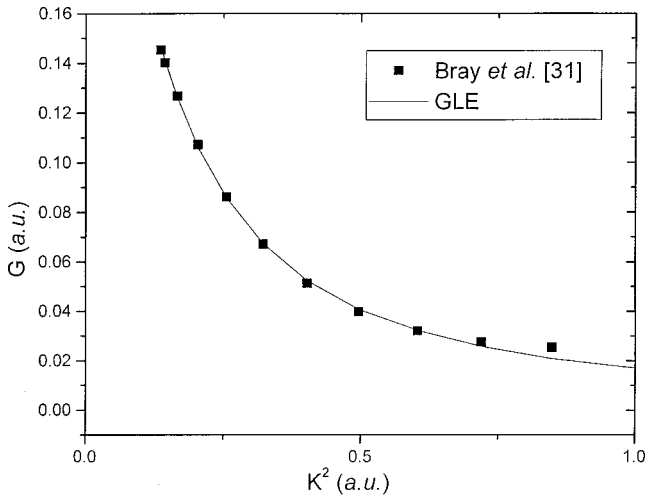

FIG. 2. Comparison of the apparent generalized oscillator strength G for H $1s$-$2p$ from the data of Bray, Konovalov, and McCarthy [31] (rectangles) and from the GLE (continuous curve) at 19.58 eV. Note the extensive nonphysical region, and that the data point at about 0.65 a.u. corresponds to $\theta=40°$.

AGOS in terms of *only three* energy-independent parameters A, C, and OOS (usually a known quantity determined independently).

The beauty of Eq. (17) is structural simplicity; it manifests directly the energy dependence of the AGOS through the second term. We refer to this second term as the ''moving Regge pole'' contribution to the AGOS. The whole expression is referred to as the generalized Lassettre expansion [30] for obvious reasons. The GLE represented by Eq. (17) differs from others [19,20] through the presence of the second term, which also contains the square root of K^2 singularity at $K^2=0$, whose importance was pointed out in Ref. [45]. The GLE was used to extract the OOS within 1% accuracy for the H $1s$-$2p$ transition from the accurate DCS's of Ref. [31]. The calculation used all the DCS data obtained at scattering angles from 0° to 90° (15 data points) for each electron-impact energy $E=19.58$, 35, 40, 54.4, 100, and 200 eV. Also, even when the data at 19.58 eV were used alone, the accuracy was still impressive, better than 1.2%.

Figures 2, 3, and 4 show the excellent agreement between the data of Ref. [31] and the GLE at 19.58, 54.4, and 200 eV, respectively. Our calculation used the values $C=12.2$ and $A=-2.98$, obtained in Ref. [30]. We note that when E is close to $\omega(E=19.58\,\text{eV})$, all the data points corresponding to $\theta\leqslant 40°$ are concentrated within a narrow range of K^2 values, viz. $0\leqslant K^2\leqslant 0.65$ a.u., while for large $E(E=200$ eV) the data $\theta\leqslant 70°$ cover a significant range $0\leqslant K^2\leqslant 30$ a.u. Also, at 200 eV the data points are well separated near $\theta=0°$ in comparison with those at $E=19.58$ or 54.4 eV. Thus, in an appropriate representation, the AGOS's can be represented by straight lines. This has allowed us to determine the unmeasured data near $\theta=0°$ for other transitions through analytical continuation. If the data at $E=200$ eV are continued to $K^2=0$, the AGOS curve intersects the vertical axis at nearly the OOS value. However, it is not obvious where the data at $E=19.58$ eV would intersect the vertical axis if analytically continued through the nonphysical region which is significant in this case.

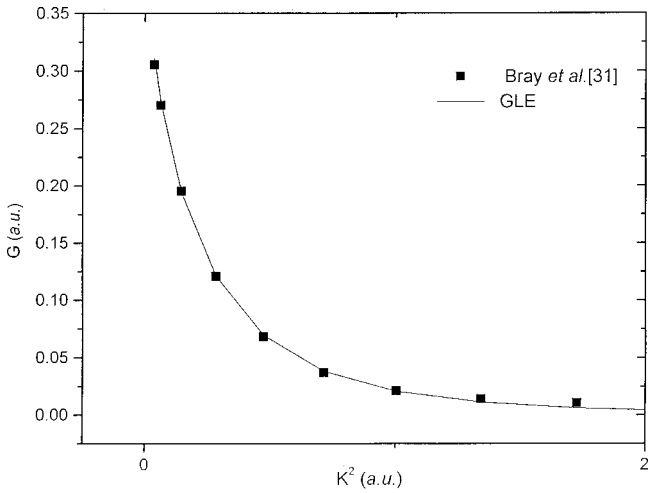

FIG. 3. Same as in Fig. 2, except that $E=54.4$ eV and the data point at about 1.75 a.u. corresponds to $\theta=40°$.

Similar results to those for H $1s$-$2p$ are obtained for the optically allowed transition Li $2\,{}^2S-2\,{}^2P^o$. Figure 5 compares the GLE results with the data from the accurate calculation of DCS's in Ref. [46] at 6, 15, and 100 eV. Here we used the values shown in Table I for the constants A and C in Eqs. (17) and (18) for each E value. The constants were determined from the data of Ref. [46] for each energy value, following Ref. [30]. Note that 6 eV is relatively medium energy (about 3ω), since for Li $2\,{}^2S-2\,{}^2P^o$, $\omega=1.8470$ [47]. Also, 100 eV is fairly high energy because $E=54\omega$. From the data of Ref. [46], the OOS can be calculated using a single energy value as in Table I, or globally [30]. The value of 0.800 obtained from the 100-eV data is slightly higher than the most recent theoretical value of 0.7470 [47],

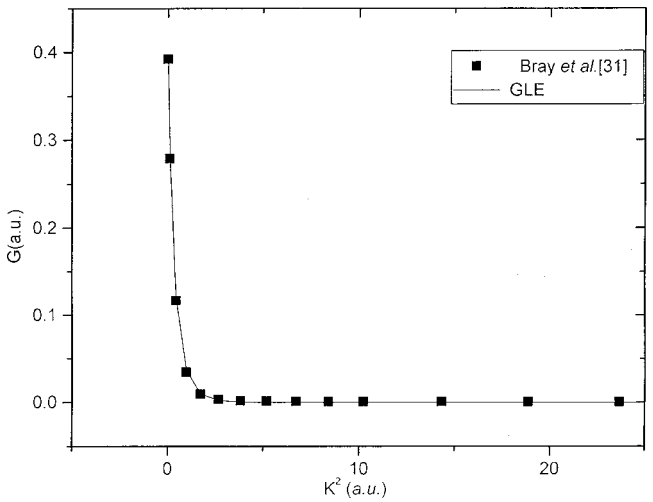

FIG. 4. Same as in Fig. 2, except that $E=200$ eV and the data point close to 30 a.u. corresponds to $\theta=70°$. Note that the nonphysical region has almost completely disappeared, and that the data at large K^2 are on the $G=0$ line and at small K^2 values they are nearly parallel to the $K^2=0$ axis and cross at almost the OOS value if analytically continued to $K^2=0$.

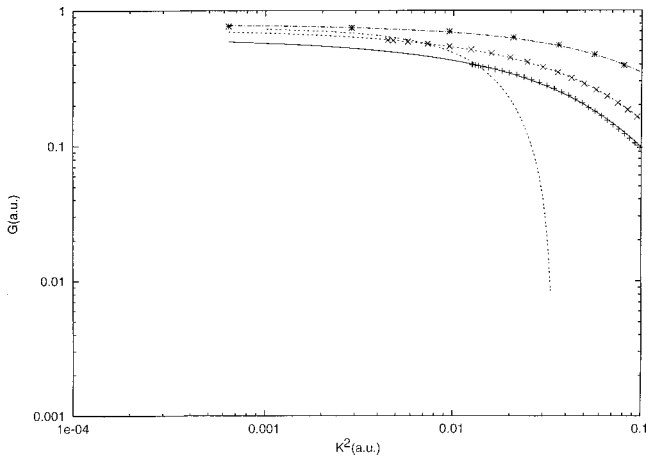

FIG. 5. Comparison of the apparent generalized oscillator strength G vs K^2 for Li $2\ ^2S-2\ ^2P^o$ from the data of Bray, Fursa, and McCarthy [46] and the GLE. Also included is the FSF curve (-- --). The pluses, crosses, and stars, together with their corresponding GLE curves, are at 6, 15, and 100 eV, respectively. The FSF, as expected, connects the $\theta=0°$ points of the $E=6$, 15, and 100 eV data points, within the calculational errors. The GLE curves have been extended into the nonphysical regions of the 6- and 15-eV data by allowing them to cross the FSF curve. Absolute data must terminate on the FSF curve.

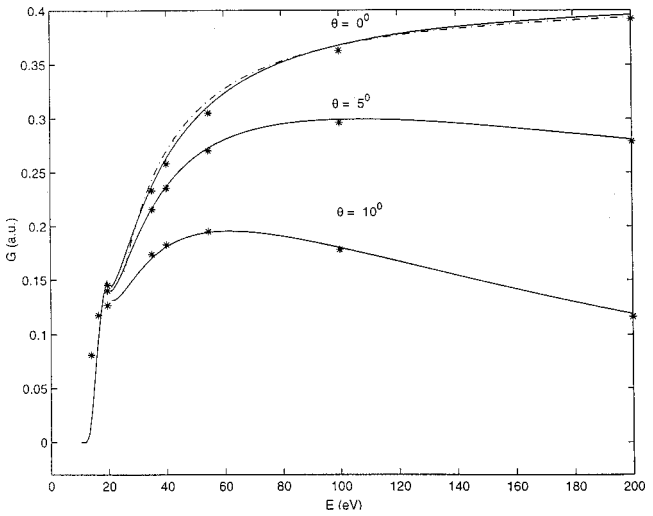

FIG. 6. Comparison of the apparent generalized oscillator strength G for H $1s$-$2p$ as a function of E from the data of Bray, Konovalov, and McCarthy [31] (**) and the GLE (—) at $\theta=0°$, 5°, and 10°. Near $E=\omega$ ($E\leqslant 20$ eV, approximately) the data corresponding to $\theta=0°$, 5°, and 10° become indistinguishable, as required by the kinematics of Fig. 1. Also included is the FSF (-•-).

and the experimental values whose range is between 0.742 and 0.750 [48]. The reason why the OOS's obtained from the 6- and 15-eV data are low is clear from Fig. 6; the values at $\theta=0°$ terminate at slightly lower values than those required by the FSF. Hence the lower values of the OOS's. It is seen that the GLE provides a powerful and simple method of determining OOS's from absolute electron DCS's even when the impact energy is near threshold. For H $1s$-$2p$ we saw that at 19.58 eV (1.9 ω) the OOS value was obtained to within 1.2% using the GLE [30], while for Li $2\ ^2S-2\ ^2P^o$ the accuracy is within 15% at $E=3\omega$. We note that the accuracy of the determined OOS value depends on that of the calculated or measured DCS's. To our knowledge the GLE is the only method available that is currently capable of such an outstanding feat.

Some remarks are appropriate here concerning the representation used for the H $1s$-$2p$ and Li $2\ ^2S-2\ ^2P^o$ data in Figs. 2–4 and 5, respectively. Note that the data for H and Li are represented using a linear and a log graph paper, respectively and for both transitions the GLE agrees excellently with the data of Bray and co-workers [31,46]. It is clear from Fig. 5 that analytically continuing the data at 6 and 15 eV through the extensive nonphysical region of the AGOS's may not lead to the OOS value at $K^2=0$, consistent with the observation of Ester and Kessler [12] for Xe. However, the inclusion of the FSF ensures that the data terminate properly within the experimental or calculational errors, provided that they are absolute; otherwise they must be shifted up or down for compatibility with the FSF. The important point here is that the GLE agrees with the accurate data down to near threshold. Figure 5 also shows that within the selected range 0.0006–0.1 a.u. of K^2 values, the 100-, 15-, and 6-eV curves contain seven, 18, and 29 angular data points, respectively. This behavior is consistent with the data of Figs. 2–4 and is general. The choice of the representation will depend mainly on the objective. The log×log plots demonstrate the self-consistency of the data; properly normalized data must terminate on the FSF at values of K^2 corresponding to $\theta=0°$ at every impact energy and curves never cross.

TABLE I. Determined constants A, C, and f^0 for the Li $2\ ^2S-2\ ^2P^o$ transition from the data of Ref. [46]. Note that here the constants are determined for each impact energy rather than globally as was done for H $1s$-$2p$.

E (eV)	ν	A	C	f^0
6	9.28	12.5162	−2.2200	0.637
15	8.26	38.3503	−2.1258	0.744
100	6.04	8.6270	−0.9284	0.800

III. LASSETTRE LIMIT THEOREM

In this section we demonstrate the validity of the Lassettre limit theorem, viz. $\lim_{K^2\to 0} f(E,K^2)=f^0$, regardless of the electron-impact energy. Figure 1 shows that the $\theta=0°$ curve is the only fixed scattering angle trajectory that connects continuously $E=\omega(t=1)$ and $E=\infty(t=0)$, the OOS limit, without traversing the nonphysical region. Trajectories at any other fixed angle cannot lead to the OOS limit, although all begin at $t=1$. For example, the 10° curve clearly avoids the OOS limit as $E\to\infty$. We note that although the second curve, called the envelope curve [32], also connects $E=\omega$ and $E=\infty$ continuously, but it does not do so at a fixed angle. Furthermore, we saw that as $E\to\omega$, the angular dependence of Eq. (10) is eliminated; all the small angular curves merge with the $\theta=0°$ curve as $E\to\omega$. Therefore, the small-angle, approximately $\theta\leqslant 15°$ (the angular regime of

TABLE II. Determined GLE constants for the systems of interest. The values of the constants A and C in the second row of the H $1s$-$2p$ transition are from Ref. [30].

System	A	C	E_1	E_2	f^0
H $1s$-$2p$	−3.340	14.565	25.5	152.0	0.415
	−2.980	12.200			
He $1\ ^1S-2\ ^1P^o$	−1.217	0.370	24.0	84.0	0.278
Xe$[\frac{3}{2}]$	−1.827	5.262	17.0	64.0	0.230
$N_2O\ 2\ ^1\Sigma$	−27.013	481.152	17.0	65.0	0.330

interest of this paper), behavior can be approximated by that of the $\theta=0°$ curve as $E\rightarrow\omega$.

In Fig. 6 we show the AGOS versus E for the H $1s$-$2p$ transition at $\theta=0°$, 5°, and 10°. The solid curves are calculated using the values of the constants A and C obtained in Ref. [30]. The dash-dotted curve is the forward scattering function of Ref. [32], while the asterisks represent data from Ref. [31]. The agreement between the data of Ref. [31] and the GLE is excellent down to near threshold. Note that the 10° and 5° curves merge with the zero degree curves as $E\rightarrow\omega$, consistent with the kinematics, Fig. 1. As $E\rightarrow 200$ eV, the separation among the various curves becomes larger in comparison with that near $E=\omega$. That AGOS curves other than that corresponding to $\theta=0°$ must vanish as $E\rightarrow\infty$ follows from Eq. (17). As $E\rightarrow\infty$ the second term becomes negligible, and only the Born term survives, viz.

$$f(E,K^2)=\frac{f^0}{(1+x^2)^6}=\frac{f^0}{[1+4DE(1-\cos\theta)]^6} \qquad (19)$$

where D is a constant independent of E.

When $\theta=0°$ in Eq. (19), the $f(E,K^2)=f^0$. Therefore, the $\theta=0°$ trajectory of the AGOS is the only fixed scattering angle curve for reaching the Lassettre limit when starting from any E value, and without involving the nonphysical region. This clearly demonstrates the single-pole dominance of the scattering process at forward scattering. For any nonzero scattering angle, $f(E,K^2)\sim(\omega/E)^6$ which approaches zero as $E\rightarrow\infty$. Consequently, the $\theta=5°$ and 10° (or any $\theta\neq 0°$) AGOS curves actually go to zero as $E\rightarrow\infty$, leaving only the forward-scattering curve to satisfy the Lassettre limit theorem, consistent with the kinematics of Fig. 1. Thus establishing the applicability of the Lassettre limit theorem regardless of the electron-impact energy requires an appropriate universal representation of the kinematics and the AGOS.

Some immediate consequences of the Lassettre limit theorem are worth mentioning. From Fig. 6 it is now clear that knowing the absolute values of the DCS's at $\theta=0°$ as a function of E, the data can be used to determine the value of the OOS [5,12], the accuracy being determined by that of the DCS's. This is a superior approach because it completely avoids the extrapolation of the AGOS, particularly through the nonphysical region, and it should be contrasted with that used in Refs. [5, 12]. Experimentally, it would be easier to separate the angular dependence of the AGOS's as $E\rightarrow\infty$, rather than for those near threshold. Most importantly, the GLE at $\theta=0°$ defines the long-sought-after unique normalization curve of the AGOS's to the OOS. This implies that for absolute data, the AGOS at any impact energy must lie on this curve; otherwise the data point at the given impact energy must be shifted up or down so that it is on the curve. Interestingly, it would be difficult to separate in general spuriously behaved data points from improperly normalized data points. However, the self-consistency of the data as a function of angle or K^2 can be ascertained using the MDM, as demonstrated by Felfli and Msezane [36] and Marinkovic *et al.* [37].

IV. NORMALIZATION OF DIFFERENTIAL CROSS SECTIONS

Since at zero-angle scattering the GLE connects continuously the threshold energy point and the infinite energy point (the OOS), it therefore represents the long-sought-after normalization curve to the OOS, regardless of the impact energy and without involving the nonphysical region. In this section we extract the normalization curves appropriate to the optically allowed transitions in H, He, Xe, and N_2O to demonstrate correctly normalized data and/or spuriously behaved data at or near $\theta=0°$. To analyze these transitions using the GLE we need the values of the constants A and C in the expression of the GLE. As pointed out in Ref. [30], C can be determined directly by solving the Schrödinger equation, a laborious process, or from the measured data.

One main objective of this paper is to demonstrate the applicability of the GLE. Therefore, the constants A and C will be extracted in a simple way. This is accomplished by matching at $\theta=0°$ the GLE and the FSF, including its generalized version [42], at two arbitrary impact energies, one high, E_2, and the other low, E_1. Table II shows the results of such a determination. The constants are not too sensitive to the choice of E_1 and E_2 as long as they are reasonably separated. We note that, while the FSF can be used only at $\theta=0°$, the GLE can also be employed for $\theta\neq 0°$, as shown in Fig. 6. The curves at $\theta=0°$, 5°, and 10° were obtained using the same constants from Ref. [30], given in Table II. Also, the GLE can be used to determine OOS's [30].

Unlike for the H $1s$-$2p$ transition, there are many measurements and calculations of the DCS's for the He $1\ ^1S-2\ ^1P^o$ transition at and near $\theta=0°$, the angular region of our interest. Since in this paper we want to demonstrate the applicability of the GLE, we have selected the measurements [49–52] and calculations [52–54]. Combined, they cover the electron-impact energy range $23.2\leqslant E\leqslant 1500$ eV,

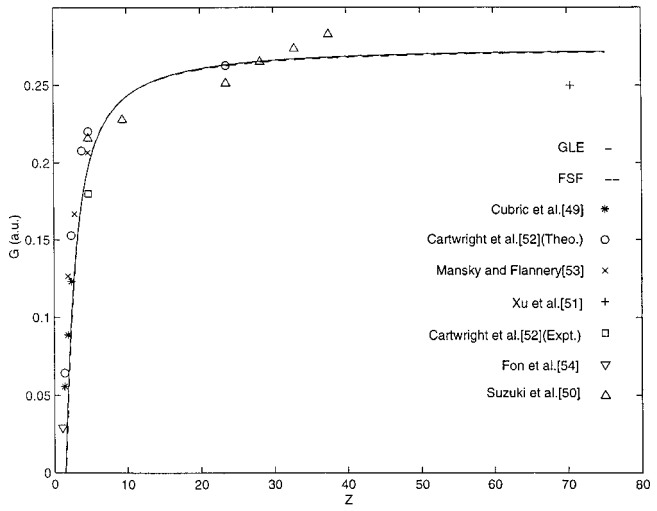

FIG. 7. The apparent generalized oscillator strength G for He $1\ ^1S-2\ ^1P^O$ from the GLE (—) and FSF ($-\ -\ -$) are compared with those from various measurements [49–52] and calculations [52–54]. The variable $Z=E/\omega$ is used for the horizontal axis.

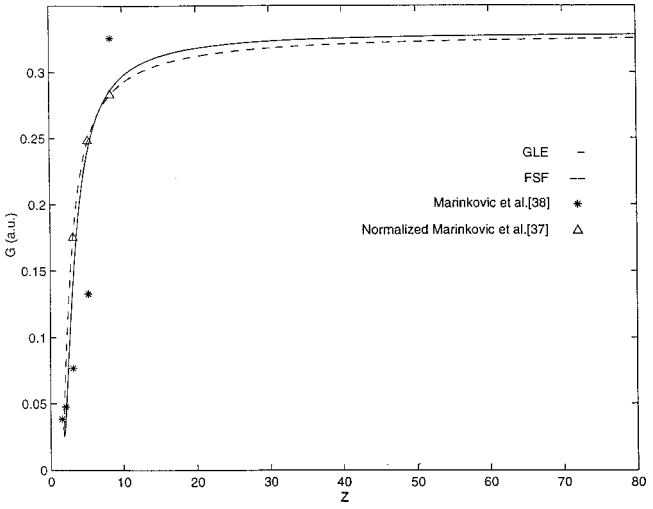

FIG. 9. Same as in Fig. 8, except that the data are for the excitation of the $2\ ^1\Sigma$ state of N_2O and the measurements are from Marinkovic and co-workers [37,38].

and the angular regime $0°\leqslant\theta\leqslant180°$. Because of the availability of the measured data at and near $\theta=0°$, the four measurements are suitable for demonstrating the normalization capability of the GLE. We define the scaled energy as $Z=E/\omega$.

In Fig. 7 various selected calculations [52–54] and measurements [49–52] of the AGOS's at $\theta=0°$ for He $1\ ^1S-2\ ^1P^o$ are compared with the GLE and FSF curves for $23.2\leqslant E\leqslant1500$ eV. The results demonstrate that the GLE can be employed to normalize relative measurements to the OOS at any E, and/or assess the reliability of measured or calculated electron DCS's at $\theta=0°$, even very close to threshold. We obtained the AGOS's at $\theta=0°$ for $E=100$ and 1500 eV for the measured data [50,51] using the MDM, because the last measurements were at 1.2° and 2°, respectively. Although the data point of Xu *et al.* appears significantly lower than the FSF and GLE curves, it is, nevertheless within the experimental errors. Also, the measurement [50] appears to be increasing away from the OOS limit as E increases from 600 to 800 eV. This behavior is incorrect, but is still within the experimental errors. Just like for the H $1s$-$2p$ transition, the GLE represents very well the measured He $1\ ^1S-2\ ^1P^o$ data over a wide range of E values.

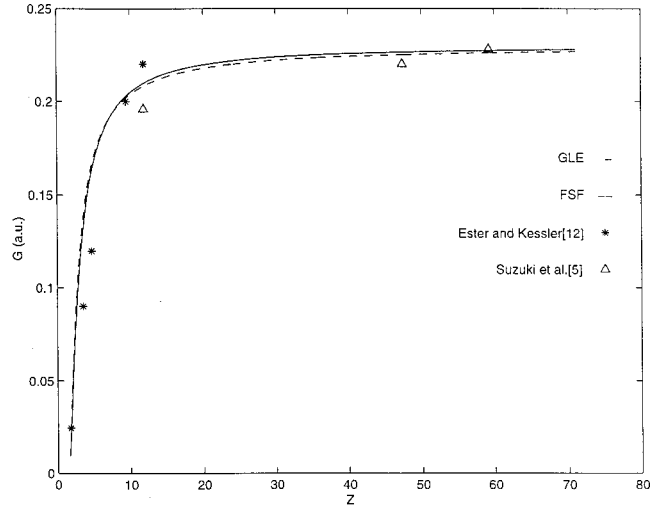

FIG. 8. Comparison of the apparent generalized oscillator strength G as a function of Z for the excitation of the Xe$[\frac{3}{2}]6s$ state from the GLE (—) and FSF ($-\ -\ -$), with data from the measurements of Suzuki *et al.* [5] and Ester and Kessler [12].

Suzuki *et al.* [5] measured the electron excitation DCS's for Xe $[\frac{3}{2},\frac{1}{2}]6s$ states from ground state at 100, 400, and 500 eV, down to scattering angles $\theta_s=2.45°$, 1.4°, and 1.5°, respectively. Ester and Kessler [12] measured absolute DCS's for the same transitions at E values between 15 and 100 eV, but only down to $\theta_s=6°$. Both experiments also determined OOS's. Ester and Kessler also demonstrated that their data at 100 and 80 eV were compatible with Lassettre's limit theorem, while those for $E\leqslant40$ eV were not. To apply the GLE to both measurements, we must first obtain data at $\theta=0°$ from the respective data sets using the MDM. Within the experimental errors, the data points at $\theta=0°$ must lie on the corresponding GLE curve as in Fig. 6. Figure 8 compares Suzuki *et al.*'s [5] data with that of Ester and Kessler for the Xe $[\frac{3}{2}]6s$ state. The GLE and FSF curves are also included, and are in good agreement with the measurements within their errors. We note that Khakoo *et al.* [55] also measured DCS's for features 1 and 2 of Xe for $0°\leqslant\theta\leqslant180°$ at 15, 20, and 30 eV. However, their data for feature 2 are ill behaved near $\theta=0°$ at 15 and 20 eV; the rest of their data behave excellently.

Marinkovic *et al.* [38] measured electron DCS's for excitation of the $2\ ^1\Sigma$ and $^1\Pi$ states of N_2O from the ground state. Relative measurements were obtained at 50, 40, 30, and 15 eV, and absolute data at 80 eV down to $\theta=0°$. The measured data were recently normalized through GOS's [37] using the FSF [32]. Before the normalization was effected at each E, the reliably measured larger angular data were analytically continued using the MDM to obtain data at θ

$=0°$, and to identify spurious behavior. The data were then normalized, after correction to the OOS, following Felfli and Msezane [36]. Figure 9 displays both unnormalized and normalized data at $\theta=0°$ for the $2\ ^1\Sigma$ state of N_2O at 80, 50, 40, 30, and 15 eV. Also included are the GLE and FSF curves. As can be seen, the agreement between the two curves is very good down to near threshold. Figure 9 demonstrates how the GLE can be used to normalize relative measurements for a molecular transition.

V. CONCLUSION AND DISCUSSION

The most important accomplishment of this paper has been to apply the GLE to H $1s$-$2p$, to demonstrate that only at $\theta=0°$ does the AGOS continuously connect the threshold energy and the infinite energy points without the involvement of the nonphysical region; the latter limit corresponds to the OOS. To our knowledge, this is the first demonstration of the applicability of the Lassettre limit theorem regardless of the electron-impact energy. The limit theorem has been always attractive to experimenters for normalizing their relative measurements of electron DCS's to the OOS. Here, using optically allowed transitions in H, He, Xe, and N_2O, we have shown that the GLE at $\theta=0°$ can be used not only to ascertain correctly normalized measured electron DCS's but also to identify and correct spuriously behaved data near and at $\theta=0°$, regardless of the electron-impact energy.

However, caution must be exercised in using the GLE for normalizing relative measurements of DCS's because, currently, zero-degree measurements are almost nonexistent or are riddled with errors. Accurate DCS's at small scattering angles, including zero, are important for the determination of integral cross sections since this angular regime contributes significantly to them. The MDM complements the GLE since, it can analytically continue the large angular measurements, which are generally more accurately measured by comparison, through the unmeasured angular regime to $\theta=0°$. Thus it can be determined whether the data require renormalization or are spuriously behaved. The FSF is another important method, since it is simple to use, requiring only the OOS as input. As indicated in this paper, it can also be used to determine the constants A and C in the expression of the GLE, as well as to check properly normalized data through the OOS.

We conclude by noting that anomalies in the excitation threshold law, nonexistent for the typical complex atom, are introduced in the excitation of the $2p$ level of H due to the degeneracy of and asymptotic coupling between the $2s$ and $2p$ levels [56]. The problem, well discussed by Geltman [56], is currently being investigated. Suffice it to state that the GLE at $\theta=0°$ can be used to normalize relative DCS's for both atomic and molecular transitions over a wide range of electron-impact energies. Also, it is expected to provide a stringent test of both measurements and theory at and near $\theta=0°$. With some little modifications, the GLE is equally applicable to the normalization of the DDCS's for ionization by electron impact and to optically forbidden transitions. For the latter, even though the OOS is equal to 0, the curves can still be used to normalize the DCS's through the AGOS since its value is nonzero for $\omega<E<\infty$. The GLE also validates the FSF [32] over its range of applicability.

Note added. After the completion of this work, Avdonina *et al.* [57] showed that in an appropriate representation, the AGOS permits the demonstration of its general properties. They also showed that when the AGOS, from DCS measurement or calculation, was plotted against the variable u of Eq. (9), excellent agreement was obtained with the measured data of Ref. [34] and the calculation of Ref. [46] at $\theta=1°$, 3°, 5°, and 10°, but not at $\theta=0°$. At zero-degree scattering they found that the data of Ref. [34] required only multiplication by a factor of about 0.6 for compatibility with the accurate data of Ref. [46], while the data of Ref. [58] behaved spuriously (only at $\theta=0°$). Consistent with the present results of Figs. 6–9, the representation of the measured or calculated electron DCS's for optically allowed transitions used by Avdonina *et al.* [57] readily reveals improperly normalized and/or spuriously behaved data at small scattering angles, approximately $\theta\leqslant 15°$. Their analysis is also applicable even to heavy atoms such as the optically allowed transition of Ba [59]. The conclusions of that paper agree with those of the present paper. Both papers can now be used to guide the measurement of small-angle electron-scattering DCS's, particularly at $\theta=0°$ where measurements are almost nonexistent because of the difficulty of measuring them.

ACKNOWLEDGMENTS

Work was supported by U.S. DOE, Division of Chemical Sciences, Office of Basic Energy Sciences, Office of Energy Research (A.Z.M.), NASA-PACE, and the NSF. We thank Dr. Daniel Bessis and Dr. Carlos Handy for valuable discussions, as well as Dr. Aaron Temkin for pointing out the anomalous behavior in H $1s$-$2p$ near threshold.

[1] H. A. Bethe, Ann. Phys. (Leipzig) **5**, 325 (1930).
[2] W. F. Miller and R. L. Platzman, Proc. R. Soc. London, Ser. A **70**, 299 (1957).
[3] E. N. Lassettre, A. Skerbele, and M. A. Dillon, J. Chem. Phys. **50**, 1829 (1969).
[4] R. A. Bonham, J. Chem. Phys. **12**, 3260 (1962).
[5] T. Y. Suzuki, Y. Sakai, B. S. Min, T. Takayanagi, K. Wakiya, H. Suzuki, T. Inaba, and H. Takuma, Phys. Rev. A **43**, 5867 (1991).
[6] A. Skerbele and E. N. Lassettre, Chem. Phys. Lett. **51**, 424 (1978).
[7] K. N. Klump and E. N. Lassettre, Chem. Phys. Lett. **51**, 99 (1977).
[8] L. Vuskovic, L. Maleki, and S. Trajmar, J. Phys. B **17**, 2519 (1984); B. Marinkovic, V. Pejcev, D. Filipovic, I. Cadez, and L. Vuskovic, J. Phys. B **25**, 5179 (1992).
[9] S. Trajmar, W. Williams, and S. K. Srivastava, J. Phys. B **10**, 3323 (1977).

[10] B. Marinkovic, V. Pejcev, D. Filipovic, I. Cadez, and L. Vuskovic, J. Phys. B **19**, 2189 (1986).
[11] M. Ismail and P. J. O. Teubner, J. Phys. B **28**, 4149 (1995).
[12] T. Ester and J. Kessler, J. Phys. B **27**, 4295 (1994).
[13] T. Y. Suzuki, H. Suzuki, S. Ohtani, B. S. Min, T. Takayanagi, and K. Wakiya, Phys. Rev. A **49**, 4578 (1994).
[14] Zhifan Chen and A. Z. Msezane, J. Phys. B **31**, 1097 (1998).
[15] K. N. Klump and E. N. Lassettre, J. Chem. Phys. **68**, 3511 (1978).
[16] Zhifan Chen and A. Z. Msezane, Can. J. Phys. **74**, 279 (1996).
[17] E. N. Lassettre and M. A. Dillon, J. Chem. Phys. **59**, 4778 (1973).
[18] Z. Chen and A. Z. Msezane, J. Phys. B **31**, 4655 (1998).
[19] K. N. Klump and E. N. Lassettre, J. Chem. Phys. **68**, 886 (1978).
[20] A. Haffad, Z. Felfli, A. Z. Msezane, and D. Bessis, Phys. Rev. Lett. **76**, 2456 (1996).
[21] I. D. Williams, A. Chutjian, and R. J. Mawhorter, J. Phys. B **19**, 2189 (1986).
[22] C. C. Turci, J. T. Francis, T. Tyliszczak, G. G. B. de Souza, and A. P. Hitchcock, Phys. Rev. A **52**, 4678 (1995).
[23] M. A. Khakoo, M. Larsen, B. Paolini, X. Guo, I. Bray, A. Stelbovics, I. Kanic, and S. Trajmar, Phys. Rev. Lett. **82**, 3980 (1999); M. A. Khakoo, M. Larsen, B. Paolini, X. Guo, I. Bray, A. Stelbovics, I. Kanic, S. Trajmar, and G. K. James, Phys. Rev. A **61**, 012701 (2000).
[24] V. Karaganov, I. Bray, and P. J. O. Teubner, Phys. Rev. A **59**, 4407 (1999).
[25] K. Xu, Z. Zhong, S. Wu, R. Feng, S. Ohtani, T. Takayanagi, and A. Kimota, Sci. China, Ser. A. **38**, 368 (1995).
[26] Zhifan Chen and A. Z. Msezane, J. Chem. Phys. **102**, 3888 (1995).
[27] D. Sokolovski, J. N. L. Connor, and G. C. Schatz, Chem. Phys. Lett. **238**, 127 (1995).
[28] J. N. L. Connor, J. Chem. Soc., Faraday Trans. **86**, 1627 (1990).
[29] V. De Alfaro and T. Regge, *Potential Scattering* (North-Holland, Amsterdam, 1965).
[30] Z. Felfli, A. Z. Msezane, and D. Bessis, Phys. Rev. Lett. **81**, 963 (1998).
[31] I. Bray, D. A. Konovalov, and I. E. McCarthy, Phys. Rev. A **44**, 5586 (1991).
[32] N. Avdonina, Z. Felfli, and A. Z. Msezane, J. Phys. B **30**, 2591 (1997).
[33] M. Inokuti, Rev. Mod. Phys. **43**, 297 (1971).
[34] L. Vuskovic, S. Trajmar, and D. F. Register, J. Phys. B **15**, 2517 (1982).
[35] Zhifan Chen and A. Z. Msezane, Phys. Rev. A **55**, 812 (1997).
[36] Z. Felfli and A. Z. Msezane, J. Phys. B **31**, L165 (1998).
[37] B. Marinkovic, R. Panajotovic, Z. D. Pesic, D. M. Filipovic, Z. Felfli, and A. Z. Msezane, J. Phys. B **32**, 1949 (1999).
[38] B. Marinkovic, Cz. Szmytkovwski, V. Pejcev, D. Filipovic, and L. Vuskovic, J. Phys. B **19**, 2365 (1986).
[39] S. Wang, S. Trajmar, and P. W. Zetner, J. Phys. B **27**, 1613 (1994).
[40] A. Z. Msezane, Z. Felfli, and Z. Chen, J. Phys. B **29**, L817 (1996).
[41] A. Z. Msezane and D. Bessis, J. Phys. B **30**, 445 (1997).
[42] N. Avdonina, Z. Felfli, and A. Z. Msezane, J. Phys. B **32**, 5179 (1999).
[43] D. Vrinceanu, A. Z. Msezane, and D. Bessis, Chem. Phys. Lett. **311**, 395 (1999).
[44] D. Vrinceanu, A. Z. Msezane, and D. Bessis, Phys. Rev. A **62**, 022719 (2000).
[45] W. M. Huo, J. Chem. Phys. **60**, 3544 (1974).
[46] I. Bray, D. V. Fursa, and I. E. McCarthy, Phys. Rev. A **47**, 1101 (1993).
[47] Zong-Chao Yan and G. W. F. Drake, Phys. Rev. A **52**, R4316 (1995).
[48] A. Gaupp, P. Kuske, and H. J. Andrä, Phys. Rev. A **26**, 3351 (1982); J. Carlsson and L. Sturesson, Z. Phys. D: At., Mol. Clusters **14**, 281 (1989); W. I. McAlexander, E. R. I. Abraham, N. W. M. Ritchie, C. J. Williams, H. T. C. Stoof, and R. G. Hulet, Phys. Rev. A **51**, R871 (1995).
[49] D. Cubric, D. J. L. Mercer, J. M. Channing, G. C. King, and F. H. Read, J. Phys. B **32**, L45 (1999).
[50] T. Y. Suzuki, H. Suzuki, F. J. Currell, S. Ohtani, Y. Sakai, T. Takayanagi, and K. Wakiya, Phys. Rev. A **57**, 1832 (1998).
[51] K. Z. Xu, R. F. Feng, S. L. Wu, Q. Ji, X. J. Zhang, Z. P. Zhong, and Y. Zheng, Phys. Rev. A **53**, 3081 (1996).
[52] D. C. Cartwright, G. Csanak, S. Trajmar, and D. F. Register, Phys. Rev. A **45**, 1602 (1992).
[53] E. J. Mansky and M. R. Flannery, J. Phys. B **23**, 4573 (1990).
[54] W. C. Fon, K. P. Lim, and P. M. J. Sawey, J. Phys. B **26**, 4201 (1993).
[55] M. A. Khakoo, S. Trajmar, L. R. LeClair, I. Kanik, G. Csanak, and C. J. Fontes, J. Phys. B **29**, 3455 (1996).
[56] S. Geltman, *Topics in Atomic Collision Theory* (Klieger, Malabar, 1997).
[57] N. B. Avdonina, Z. Felfli, D. Fursa, and A. Z. Msezane, Phys. Rev. A **62**, 014703 (2000).
[58] D. H. Madison, R. P. McEachran, and M. Lehmann, J. Phys. B **27**, 1807 (1994).
[59] D. Fursa and I. Bray, Phys. Rev. A **59**, 282 (1999).